A CFD Study on Thermo-Acoustic Instability of Methane/Air Flames in Gas Turbine Combustor

Chae Hoon Sohn*
Department of Aerospace Engineering, Chosun University, Gwangju 501-759, Korea
Han Chang Cho
Research Institute of Industrial Science and Technology, San 32 Hyoja-dong, Nam-gu, Pohang 790-600, Korea

Thermo-acoustic instability of methane/air flames in an industrial gas-turbine combustor is numerically investigated adopting CFD analysis. The combustor has 37 EV burners through which methane and air are mixed and then injected into the chamber. First, steady fuel/air mixing and flow characteristics established by the burner are investigated by numerical analysis with single burner. And then, based on information on the flow data, the burners are modeled numerically via equivalent swirlers, which facilitates the numerical analysis with the whole combustion system including the chamber and numerous burners. Finally, reactive flow fields within the chamber are investigated numerically by unsteady analysis and thereby, spontaneous instability is simulated. Based on the numerical results, scaling analysis is conducted to find out the instability mechanism in the combustor and the passive control method to suppress the instability is proposed and verified numerically.

Key Words : Thermo-Acoustic Instability, Gas-Turbine Combustor, Burners, Spontaneous Instability

1. Introduction

Pressure oscillation frequently occurs in various combustors and usually affects the combustor operation unfavorably. Especially, High-performance operation of an industrial gas-turbine combustor is often impeded by thermo-acoustic instability, one kind of combustion instabilities (Lefebvre, 1998; Williams, 1985). Thermo-acoustic instability results from sound-wave amplification in a combustor, and thereby it has long gained significant interest in propulsion and power systems.

* Corresponding Author,
E-mail : chsohn@chosun.ac.kr
TEL : +82-62-230-7123; **FAX** : +82-62-230-7123
Department of Aerospace Engineering, Chosun University, Gwangju 501-759, Korea. (Manuscript **Received** February 16, 2005; **Revised** July 20, 2005)

Under thermo-acoustic instability, pressure oscillations are amplified through in-phase heat addition/extraction from combustion, leading to the acoustic resonance at the specific acoustic modes of the chamber (Harrje and Reardon, 1972; Zucrow and Hoffman, 1977). It may lead to an intense pressure fluctuation as well as excessive heat transfer to combustor wall in combustion systems such as solid and liquid propellant rocket engines, ramjets, turbojet thrust augmentors, utility boilers, and furnaces (McManus et al., 1993; Moon et al., 2004; Seo, 2003).

In order to understand this phenomenon better, detailed and extensive information on reactive flow field in the combustor is required. In this point of view, numerical researches are informative rather than experimental work since the latter still gives limited flow data in spite of formidable expense spent on full-scale test. So far, there have been conducted various analytic and numerical

studies to pursue this phenomenon (Culick and Yang, 1995; Fleifil et al., 1996; Harrje and Reardon, 1972; Sohn, 2002; Sohn et al., 2004). In fundamental works, elementary physical and chemical processes have been investigated separately based on microscopic approach and thereby, useful fundamentals were obtained. On the other hand, analyses of reactive flow field in the whole combustor including all processes were conducted to simulate unstable combustion (Davoudzadeh and Liu, 2004; Flohr et al., 2001). The latter studies have advantages in understanding and controlling combustion instabilities from the standpoint of the macroscopic approach to the phenomena. Nevertheless, due to the complexity and breadth of the analysis, there are only a few numerical studies devoted to the macroscopic approach and intended to obtain information on instability control with the whole combustor of actual size.

In this regard, the macroscopic numerical approach is adopted in this study, where cost-effective analyses are proposed and conducted for better understanding of instability mechanism and its control. Since thermo-acoustic instability occurs at frequencies close to acoustic eigenmodes of the chamber, in the previous work (Sohn and Cho, 2004), the purely acoustic analysis was carried out with the real actual-size chamber and its acoustic characteristics were found. However, chemically reacting flow and interactions between heat release and pressure oscillation were not considered in the work. Here, with reacting flow considered, combustion instabilities are simulated numerically and attention is focused on fuel/air injection and chemical-reaction processes since the only device to trigger instability is the burner mounted to the gas-turbine combustor. The instability mechanism is analyzed extensively from the numerical data. Finally, a passive control method to suppress the instability is proposed and numerically verified.

2. Numerical Methods and Models

The adopted combustion chamber is GT11N2 Silo combustor (Aigner and Müller, 1993; Lefebvre, 1998), which is in current operation and have encountered unstable combustion depending on the operating condition. The geometry and dimension of the selected combustor are shown in Fig. 1, which are the same as adopted in the previous work (Sohn and Cho, 2004). Methane and air (21% O_2/79% N_2) are adopted as fuel and oxidizer, respectively.

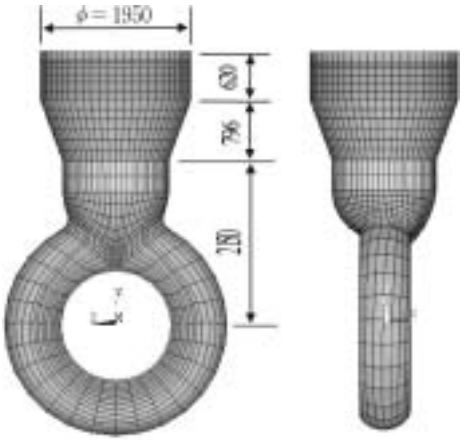

(a) Front view (b) Side view

Fig. 1 Geometries of gas-turbine combustor

2.1 Numerical methods

Numerical analysis of reactive flow field in the combustion chamber can be carried out by solving the general conservation equations for the mass, momentum, energy, and species and equation of state. In analyzing turbulent reactive flow field established in the whole combustor, direct numerical simulation is not available, but Reynolds-averaged Navier-Stokes (hereinafter, RANS) simulation is adopted here. Although Large Eddy Simulation (LES) shows better results generally, unsteady RANS are acceptably accurate and cost-effective for pressure oscillation predictions compared with 3-D LES (Cannon et al., 2001).

In averaging the conservation equations for RANS, source terms are generated which are composed of the turbulent quantities such as turbulent kinetic energy and dissipation rate, etc. Depending on the turbulence model, the mathematical formulation of the transport equations for the turbulent quantities has several versions. In

this study, standard $k-\varepsilon$ model is adopted for the simplicity (CFDRC 2003; Ferziger and Peric, 1996). In addition, to evaluate chemical-reaction term reasonably with RANS, turbulent combustion modeling, i.e., modeling of mean production rate of each species is required. Here, the eddy-breakup model is adopted (Magnussen and Hjertager, 1976; Williams, 1985). The complete formulations for RANS are omitted here and can be found in numerous literatures (Ferziger and Peric, 1996; Peters, 2000; Poinsot and Veynante, 2001). The appropriate boundary conditions for the conservation equations are discussed in the later section.

One-step chemistry, $CH_4+2O_2 \rightarrow CO_2+2H_2O$, is employed for methane-air chemical reaction and its reaction rate is expressed by the Arrhenius form,

$$k_{CH4}=-8.3\times10^5 \exp(-15098/T)\,[CH_4]^{-0.3}[O_2]^{1.3} \quad (1)$$

where the rate is expressed in unit of gmol/cm^3-s (Westbrook and Dryer, 1981). Thermodynamic and transport properties are evaluated as mixture-averaged values, but constant Prandtl and Schmidt numbers are adopted for simplicity.

For spatial discretization of the partial differential equations, central difference scheme is employed and Crank-Nicolson method is used for time integration. Thus, the second-order accuracies are guaranteed in both space and time. The coupled system of equations is solved simultaneously by using SIMPLEC algorithm. CFD-ACE+ is used to solve the generalized governing equations aforementioned and more details on numerical methods can be found elsewhere (CFDRC, 2003).

2.2 Models

The selected combustor has 37 conical premix burner modules, called the EV-burner (Lefebvre, 1998) as shown in Fig. 2. Each burner is formed by two offset half cones which are shifted to form two-diametrically-opposed air inlet slots of constant width. Gaseous fuels are injected into the air flowing into the slots by means of two fuel distribution tubes containing rows of 25 small holes with its diameter of 2.5 mm (fuel stage 2)

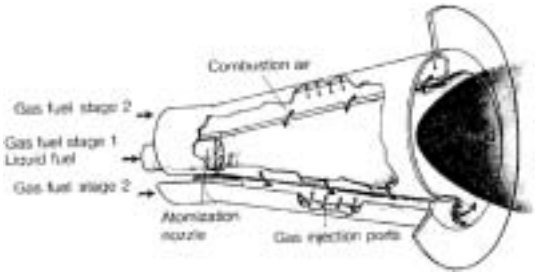

Fig. 2 Schematic of EV conical premix burner (Lefebvre, 1998)

which inject the fuel across the air stream. It has been found that mixing of fuel and air is obtained shortly after injection and the swirling mixture flows out of the cone and into the flame zone established in the chamber. In this burner, flame stabilization is accomplished in free space near the burner exit due to the sudden breakdown of a swirling flow. Although this burner can operate on both gaseous and liquid fuel, only gaseous fuel is used here. Thus, gaseous methane is injected at the apex of the cone with its diameter of 1.2 mm (fuel stage 1) as well as through 50 small peripheral holes (fuel stage 2). The inner diameters of the burner at the inlet of fuel stages and the exit are 52 mm and 130 mm, respectively. The width of channel through which the combustion air flows is 18 mm and the burner length is 335 mm. The injection velocities and thermodynamic states of fuel and air depend on the operating conditions.

The whole combustor including 37 burners considered as computational domain ranges from the burner exit to the end of flame tube as shown in Fig. 3, which corresponds to a part of the complete combustor shown in Fig. 1. The diameters of the burner-exit plane and the end outlet are 1950 mm and 1370 mm, respectively, and the longitudinal length is 1832 mm.

2.3 Numerical strategy

Combustion instability can be triggered by numerous processes such as injection, atomization, vaporization, mixing, and chemical reaction. In this combustor, gaseous fuel and oxidizer are adopted and they are mixed in the premix burner.

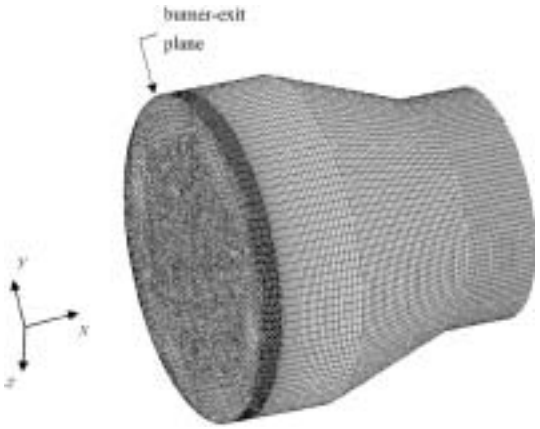

Fig. 3 Geometry and computational grids of the whole combustor with modeled swirler for combustion-instability simulation (the origin is located at the center of burner-exit plane)

Accordingly, injection into the chamber and chemical reaction are key processes here and carefully dealt with. Furthermore, since characteristic chemical-reaction time is much shorter than characteristic flow or convection time by $O(10^{-3}\sim10^{-2})$ even in lean flame (Sohn and Chung, 2000), slower processes, i.e., injection and its subsequent convection processes would be dominant over the reaction in triggering or suppressing the instability. If flow or convection time is comparable with acoustic time, which is the reciprocal of acoustic frequency of pressure oscillation, this dominance will be apparently evident. The hypothesis will be verified in the later section.

Basically, the whole combustor including 37 burners should be simulated numerically and vast numerical calculations are required. However, because of a large number of burners and their complex geometries, more effective computational strategy is proposed here without losing the essential feature of the reactive flow field.

As expected, flow field established by fuel and air injected from each burner has its own complicated mixing/flow pattern, but all the burners with the same specification would show the nearly identical flow pattern. Thus, each burner is replaced by the swirler with the similar characteristics to those of the burner in order to facilitate numerical calculation and reduce computational complexity. Consequently, the present numerical analyses are divided into two parts. As the first step, single burner is simulated numerically and the steady-state mixing and flow characteristics are investigated. Based on these data, the swirler is modeled on the burner. Next, the whole combustor, to which 37 modeled swirlers is mounted, is simulated. In simulating unstable combustion with the whole combustor, the unsteady analysis is required. Thus, the numerical simulations of combustion instability are carried out in two stages. First, the quasi-steady reactive flow field in the combustor is calculated for the given operating condition. Once the quasi-steady solution is obtained, the transient solution is sought as a function of time with the initial condition of the quasi-steady solution. Since the quasi-steady solutions include intrinsic errors and are perturbed by starting unsteady analysis, instability can be triggered spontaneously if the quasi-steady solutions are dynamically unstable (Drazin, 1992).

The thermo-acoustic response is monitored by calculating the instantaneous pressure at the representative points in the chamber. The numerical stability of the temporal integration has been checked carefully and the time step and the duration of the computation are determined depending on the acoustic frequencies, i.e., the resonant frequencies of pressure oscillation in this chamber to be investigated. Considering the dimension of the chamber, the major frequencies are predicted to be of $O(10^2\,\mathrm{Hz})$, which corresponds to $O(1\,\mathrm{ms})$ in the period. Considering this point, the usual step size is taken as $O(1\sim10\,\mu\mathrm{s})$ and the temporal integration lasts for $O(10\,\mathrm{ms})$ so as to simulate several cycles of oscillation.

3. Results and Discussions

3.1 Combustion-instability simulation

3.1.1 Flow calculation with single burner

In this study, one nominal operating condition is adopted for numerical analysis, which is sum-

marized in Table 1. The modeled geometry and computational grids of single burner are shown in Fig. 4. The interior domain of the burner is composed of unstructured grids and the whole domain consists of 150000 cells. Grid dependency of the solution has been checked compared with the solutions with 300000 cells and it has been found that the present computational grids offer accurate solution with negligible error.

As a result of cold-flow calculation without combustion, axial-velocity magnitude field is shown in Fig. 5. Recirculation zone is established away from the burner exit due to the sudden breakdown of the swirling flow at the exit, which contributes to flame holding or stabilization as already known. For swirler modeling, the mean velocities in each direction, i.e., axial velocity, u radial velocity, v, and tangential velocity, w are extracted from the numerical results. For example, the axial-velocity profiles are shown in Fig. 6.

In recirculation zone, flame would be established and the flow characteristics near flame front are known to have significant influence on triggering the instability since near-extinction flames are sensitive to external perturbation (Anderson et al., 1995; Fleifil et al., 1996; Kim and Williams, 1994; Lieuwen et al., 2001; Richards and Janus, 1998). Thus, in modeling swirler, the most noticeable point to be kept is to realize the recirculation zone reasonably. The stand-off distance of flame front from the burner exit is known as 0.1~0.2 m from the experimental observation although not described in detail here. Since swirler has simpler geometry than the actual burner and the single representative value of flow velocity in each direction is specified rather than the actual velocity profile, mass flow rate supplied

Table 1 Boundary conditions for single-burner calculation

	inlet		outlet
	fuel (methane)	oxidizer (air)	
injection velocity [m/s]	120	70	
temperature [℃]	50	380	extrapolated
pressure [Pa]	9.5×10^5	9.5×10^5	9.0×10^5

Fig. 4 Geometry and computational grids of single burner

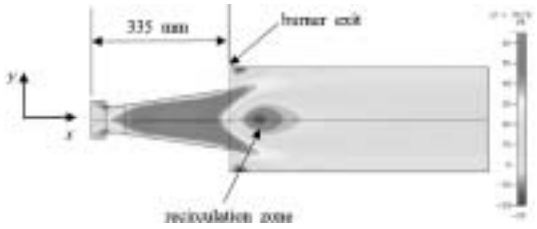

Fig. 5 Axial-velocity magnitude field from single-burner flow calculation

Table 2 Specification of modeled swirler

geometry	inner radius	70 mm
	outer radius	83 mm
mean flow velocities	axial	25 m/s
	radial	20 m/s
	tangential	60 m/s
temperature of premixture	350℃ (623 K)	
equivalence ratio	0.65	

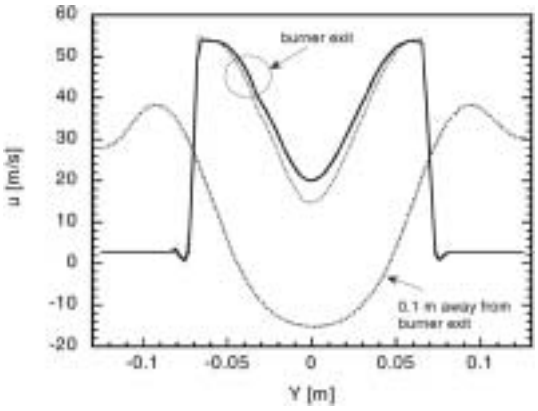

Fig. 6 Axial-velocity profiles from single-burner flow calculation

by swirler is scaled down in the ratio of 1 to 5 so as to locate the recirculation zone on the right position. The ratio is selected approximately to maintain the position in the reasonable order of magnitude. Finally, the modeled swirler has the flow specification summarized in Table 2.

3.1.2 Quasi-steady solutions calculated with whole combustor

Reactive flow field is calculated with the whole combustor including the swirlers modeled in the preceding section. The whole combustor is shown in Fig. 3. As described in section 2.3, first, quasi-steady solutions are calculated with the 32 ignited burners. Temperature field on x-y plane is shown in Fig. 7. As expected, the stand-off distance of flame front from the burner exit has $O(0.1\,\mathrm{m})$. Although not shown here, it is found that fairly homogeneous pressure filed is established from pressure-field data, but temperature field indicates distributed reaction zones leading to poor thermal efficiency. The latter phenomenon could be caused by the approximately modeled swirlers substituted for the burners and the approximate modeling of turbulent combustion. But, it affects little the instability triggering in qualitative manner since the present calculation simulates flame front reasonably.

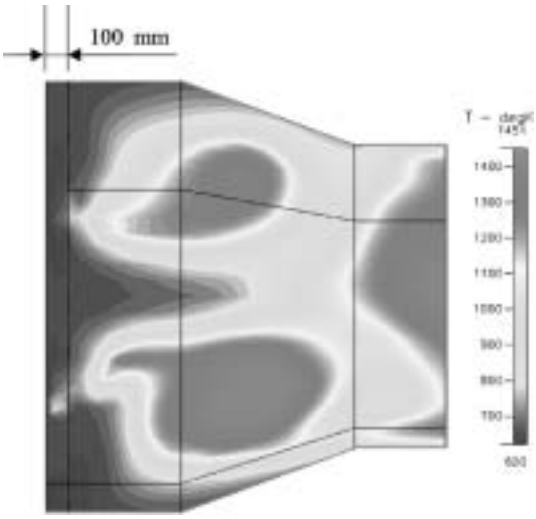

Fig. 7 Quasi-steady temperature field for nominal operating condition

3.1.3 Unsteady solutions simulating spontaneous instability

The transient solutions are calculated as a function of time with the initial condition of the quasi-steady solution as described in the preceding section. The pressure oscillation is monitored at several specified points. The transient pressure oscillations at two points of which coordinates are $(x, y, z) = (0.1, 0, 0\ \mathrm{m})$ and $(0.2, 0.3, 0\ \mathrm{m})$, respectively, are shown in Fig. 8. The data are processed by Fast Fourier Transform (hereinafter, FFT) and the transformed data or amplitude spectrums are shown in Fig. 9. The oscillating pressure has large amplitude corresponding to about 10% of the mean chamber pressure of

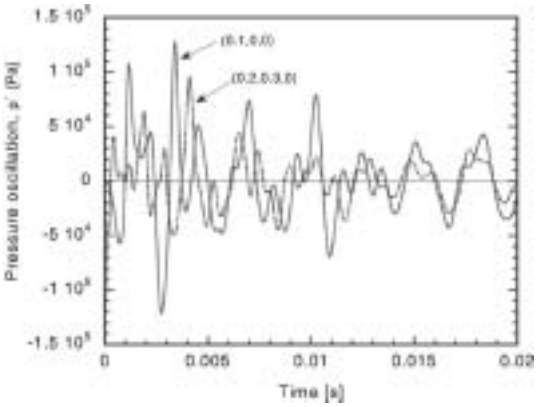

Fig. 8 Pressure oscillation as a function of time at principal monitoring points for nominal operating condition

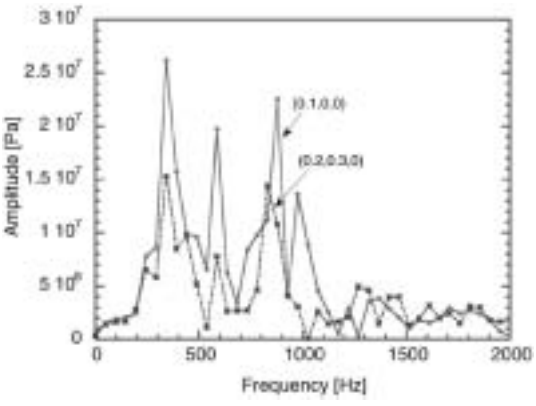

Fig. 9 Amplitude spectrum from FFT analysis for nominal operating condition

9×10^5 Pa. This large-amplitude oscillation over 5% indicates unstable combustion (Huzel and Huang, 1992).

From Fig. 9, the dominant peaks of strong oscillations are 366, 585, and 878 Hz, etc. These peaks have the similar frequencies to the measured and predicted ones in the previous work (Sohn and Cho, 2004) at which the acoustic resonance is apt to be established. This point validates the present CFD results. Here, attention is focused on lower-order acoustic modes of 366 and 585 Hz since they are triggered actually in the combustor.

3.2 Implication for suppression of combustion instability

3.2.1 Instability mechanism

From the numerical simulation, it has been found that the reactive flow field established in this combustor can trigger easily the pressure oscillation with the frequencies of $O(10^2\,\text{Hz})$. The overall triggering mechanism is investigated adopting the following scaling analysis. The key point in this analysis is that the jet flow of the premixture perturbs the flame front significantly and cause the heat-release-rate oscillation from flames.

The axial jet velocity of the premixture injected through the burner is $O(10\,\text{m/s})$ from Fig. 6 and the stand-off distance of flame front has $O(10^{-1}\,\text{m})$. Then, the characteristic jet-flow time is $O(10^{-2}\,\text{s})$ from dividing the distance by the velocity, which corresponds to the characteristic frequency, f_{jet} of $O(10^2\,\text{Hz})$. This indicates that perturbation in jet flow has the periodicity of $O(10^2\,\text{Hz})$ and thereby, the premixture is supplied to flame front periodically with the period of $O(10^2\,\text{Hz})$. Accordingly, the heat-release-rate oscillation with the same order of frequency is caused and finally, combustion instability can be triggered easily when Rayleigh criterion (Rayleigh, 1945) is satisfied because the chamber with the present geometry and dimension has the resonant frequencies of $O(10^2\,\text{Hz})$ as well.

In a similar way, Liuewen et al.(2001) suggested the following instability criterion

$$n-\frac{2}{4}<\frac{\tau_{conv,eff}}{T}<n,\ n=1,\ 2,\ \cdots \tag{2}$$

where $\tau_{conv,eff}$ denotes effective convection time of premixture and T the period of pressure oscillation. With the calculated frequencies of 366, 585, and 878 Hz, this criterion is plotted in Fig. 10. The instability regions of each mode lie in bands at various integer values of n. To locate the nominal operating point of this combustor on the instability map of Fig. 10, $\tau_{conv,eff}$ should be estimated accurately. Since $\tau_{conv,eff}$ includes chemical-reaction lag as well as convection time of premixture taken to reach the flame front from burner exit, it is defined here as

$$\tau_{conv,eff}=\frac{L_{ig}}{u_{exit}} \tag{3}$$

where L_{ig} denotes the axial distance where premixture is ignited, i.e., premixture temperature reaches spontaneous ignition temperature of about 900 K, and u_{exit} axial injection velocity of premixture jet from the burner.

With the numerical results of $L_{ig}=0.20$ m and $u_{exit}=25$ m/s, $\tau_{conv,eff}$ is estimated 8.0 ms, which corresponds to 125 Hz in period. This value of characteristic time is located on the instability map of Fig. 10 and the nominal operating condition lies in instability regions at resonant modes of 366 and 585 Hz.

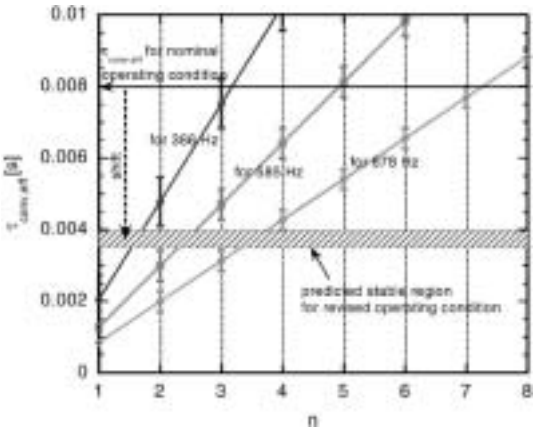

Fig. 10 Instability map on the coordinate of characteristic effective-convection time and integer, n

3.2.2 Passive control method to suppress combustion instability

To eliminate the instability, the reactive flow field should be adjusted to decouple disturbance frequencies causing high sensitivity of acoustic response from the resonant frequencies. It can be realized by changing injection velocities and/or temperature of the premixture. As a result, the stand-off distance of flame front would be adjusted and the characteristic time, $\tau_{conv,eff}$ could be shifted. As one example, if temperature is increased, the stand-off distance is shortened and $\tau_{conv,eff}$ can be shifted to lower value of 3.5~4.0 ms as indicated by the dashed arrow in Fig. 10.

To find out the temperature range of premixture corresponding to this range of $\tau_{conv,eff}$, quasi-steady calculations are repeated over the wide range of premixture temperature and $\tau_{conv,eff}$ is evaluated as a function of premixture temperature. As shown in Fig. 11, $\tau_{conv,eff}$ decreases rapidly as premixture temperature increases. From this figure and Fig. 10, the temperature range of 730 to 770 K is recommended for stable operating condition. The stability for this revised operating condition with increased temperature is verified numerically in the following section.

3.3 Numerical verification of the suppression method

For the revised condition, only premixture temperature is increased by 127 K with the other boundary conditions kept and thereby it reaches 750 K. The same calculation procedures as in sections of 3.1.2 and 3.1.3 are repeated but with temperature of 750 K. Quasi-steady temperature field is shown in Fig. 12. As predicted, the stand-off distance is shortened appreciably. From numerical data, L_{ig}=0.094 m and $\tau_{conv,eff}$ is estimated 3.8 ms, which lies in stable region as shown in Fig. 10.

As a result of unsteady analysis, pressure oscillation is plotted as a function of time in Fig. 13. Compared with Fig. 8, oscillation amplitude is

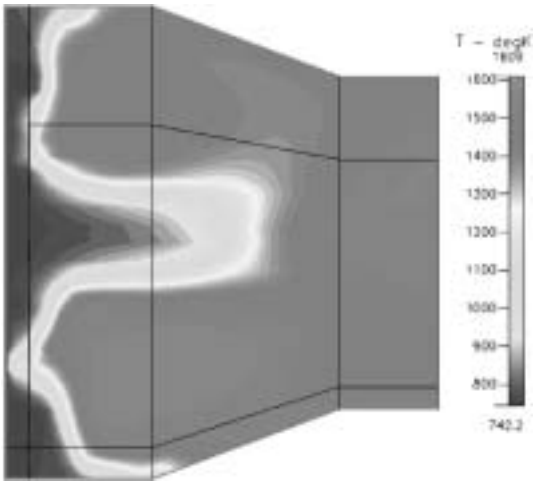

Fig. 12 Quasi-steady temperature field for revised operating condition

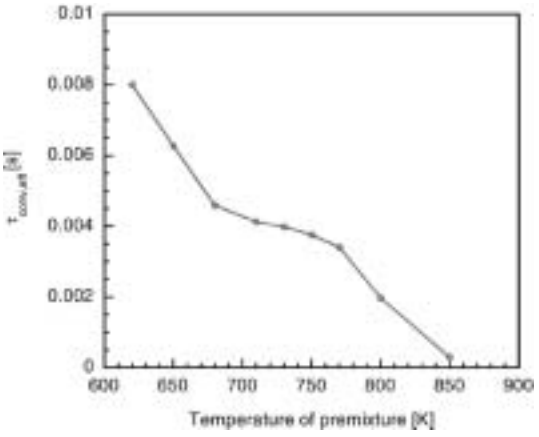

Fig. 11 Variation of effective convection time of premixture as a function of premixture temperature

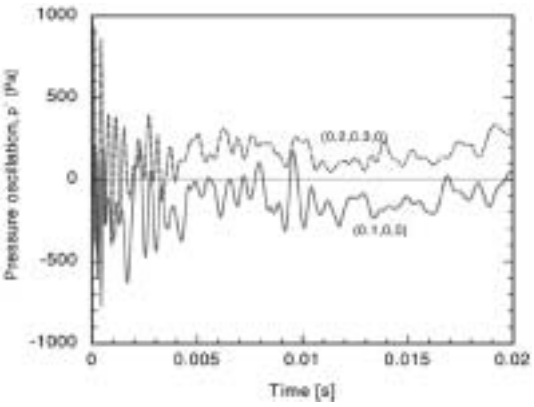

Fig. 13 Pressure oscillation as a function of time at principal monitoring points for revised operating condition

reduced appreciably and stabilized. Accordingly, the control method suggested based on the numerical data has been verified effective and viable in engineering application.

4. Concluding Remarks

Combustion instability in an industrial gas-turbine combustor encountering with undesirable pressure oscillation has been numerically investigated. Here, attention is focused on injection and its subsequent process of chemical reaction since the only device to trigger instability is the burner injecting the gaseous premixture.

As the first step for the numerical simulation of combustion instability, steady fuel/air mixing and flow characteristics established by the EV burner have been investigated by numerical analysis with single burner. And then, based on the flow data, swirler has been modeled on the burner. Finally, reactive flow fields with the whole combustor have been investigated numerically by unsteady RANS and thereby, spontaneous instability has been simulated.

In this combustor, it has been found that the heat-release-rate oscillation from the reactive flow filed is closely coupled with acoustic oscillation in the chamber, leading to strong pressure oscillation with large amplitude. The instability mechanism has been applied to find out passive control method to suppress the instability. The proposed control method has been verified effective and can be a viable method in engineering application. Accordingly, the present results can be applied for the prediction of pressure oscillation and its suppression in the gas-turbine combustor. In such a case, it is worthy of note that suitably-combined adjustment of premixture temperature, injection velocities, equivalence ratio, etc can control various aspects such as instability and performance compromisingly.

Natural gas fuels and inlet fuel/air temperatures can vary widely depending on time of year and quality of natural gas, particularly regarding the methane content. The method proposed in this study will be investigated for various fuels and wide range of fuel/air temperatures in the future work. Due to limited measurable data and experimental difficulty with whole full-scale combustor, experimental validation works using well-posed sub-scale combustor will be useful future works.

References

Aigner, M. and Müller, G., 1993, "Second-Generation Low-Emission Combustors for ABB Gas Turbines : Field Measurements with GT11N- EV," *Journal of Engineering for Gas Turbines and Power*, Vol. 115, pp. 533～536.

Anderson, W. E., Ryan, H. M. and Santoro, R. J., 1995, in *Liquid Rocket Engine Combustion Instability* (V. Yang, and W. E. Anderson, eds.), Progress in Astronautics and Aeronautics, Vol. 169, AIAA, Washington DC, pp. 215～246.

Cannon, S. M., Adumitroaie, V. and Smith, C. E., 2001, "3D LED Modeling of Combustion Dynamics in Lean Premixed Combustors," ASME paper #2001-GT-0375.

CFDRC, 2003, *CFD-ACE-GUI Modules Manual*, Vol. 1, Ver. 2003, Huntsville, AL.

Culick, F. E. C. and Yang, V., 1995, in *Liquid Rocket Engine Combustion Instability* (V. Yang, and W. E. Anderson, eds.), Progress in Astronautics and Aeronautics, Vol. 169, AIAA, Washington DC, pp. 3～38.

Davoudzadeh, F. and Liu, N., 2004, "Numerical Prediction of Non-Reacting and Reacting Flow in a Model Gas Turbine Combustion," ASME paper #2004-GT-53496.

Drazin, P. G., 1992, *Nonlinear Systems*, Cambridge Univ. Press, Glasgow, UK.

Ferziger, J. H. and Peric, M., 1996, *Computational Methods for Fluid Dynamics*, Springer-Verlag, Berlin, Germany.

Fleifil, M., Annaswamy, A. M., Ghoniem, Z. A. and Ghoniem, A. F., 1996, "Response of a Laminar Premixed Flame to Flow Oscillations : A Kinematic Model and Thermoacoustic Instability Results," *Combustion and Flame*, Vol. 106, pp. 487～510.

Flohr, P., Oliver, P., van Roon, B. and Schuermans, B., 2001, "Using CFD for Time-Delay Modeling of Premix Flames," ASME

paper #2001-GT-0376.

Harrje, D. J. and Reardon, F. H.(eds.), 1972, *Liquid Propellant Rocket Combustion Instability*, NASA SP-194.

Huzel, D. K. and Huang, D. H., 1992, *Modern Engineering for Design of Liquid-Propellant Rocket Engines*, Vol. 147, Progress in Astronautics and Aeronautics, AIAA, Washington DC, p. 113.

Kim, J. S. and Williams, F. A., 1994, "Contribution of Strained Diffusion Flames to Acoustic Pressure Response," *Combustion and Flame*, Vol. 98, pp. 279~299.

Lefebvre, A. H., 1998, *Gas Turbine Combustion*, 2nd ed., Taylor & Francis, Ann Arbor, MI.

Lieuwen, T., Torres, H., Johnson, C. and Zinn, B. T., 2001, "A Mechanism of Combustion Instability in Lean Premixed Gas Turbine Combustors," *Journal of Engineering for Gas Turbines and Power*, Vol. 123, pp. 182~189.

Magnussen, B. F. and Hjertager, B. H., 1976, "On Mathematical Modeling of Turbulent Combustion with Special Emphasis on Soot Formation and Combustion," *The Sixteenth (International) Symposium on Combustion*, The Combustion Institute, Pittsburgh, PA, pp. 719~729.

McManus, K. R., Poinsot, T. and Candel, S. M., 1993, "A Review of Active Control of Combustion Instabilities," *Progress in Energy and Combustion Science*, Vol. 19, pp. 1~29.

Moon, G. F., Lee, J. H., Jeon, C. H. and Chang, Y. J., 2004, "Experimental Study on Heat Release in a Lean Premixed Dump Combustor Using OH Chemiluminescence Images," *Transactions of KSME (B)* (in Korea), Vol. 28, No. 11, pp. 1368~1375.

Peters, N., 2000, *Turbulent Combustion*, Cambridge Univ. Press, UK.

Poinsot, T. and Veynante, D., 2001, *Theoretical and Numerical Combustion*, R. T. Edwards, Inc., Philadelphia, PA.

Rayleigh, J. W. S., 1945, *The Theory of Sound*, Vol. 2, Dover, NY. pp. 226~235.

Richards, G. and Janus, M. C., 1998, "Characterization of Oscillation During Premix Gas Turbine Combustion," *Journal of Engineering for Gas Turbines and Power*, Vol. 120, pp. 294~302.

Seo, S., 2003, "Combustion Instability Mechanism of a Lean Premixed Gas Turbine Combustor," *KSME International Journal*, Vol. 17, No. 6, pp. 906~913.

Sohn, C. H., 2002, "Unsteady Analysis of Acoustic Pressure Response in N_2 Diluted H_2 and Air Diffusion Flames," *Combustion and Flame*, Vol. 128, pp. 111~120.

Sohn, C. H. and Cho, H. C., 2004, "Numerical Analysis of Acoustic Characteristics in Gas Turbine Combustor with Spatial Non-homogeneity," *KSME International Journal*, Vol. 18, No. 8, pp. 1461~1469.

Sohn, C. H. and Chung, S. H., 2000, "Effect of Pressure on the Extinction, Acoustic Pressure Response, and NO Formation in Diluted Hydrogen-Air Diffusion Flames," *Combustion and Flame*, Vol. 121, pp. 288~300.

Sohn, C. H., Seol, W. -S., Shibanov, A. A. and Pikalov, V. P., 2004, "On the Method for Hot-Fire Modeling of High-Frequency Combustion Instability in Liquid Rocket Engines," *KSME International Journal*, Vol. 18, No. 6, pp. 1010~1018.

Westbrook, C. K. and Dryer, F. L., 1981, "Simplified Reaction Mechanisms for the Oxidation of Hydrocarbon Fuels in Flames," *Combustion Science and Technology*, Vol. 27, pp. 31~43.

Williams, F. A., 1985, *Combustion Theory*, 2nd ed., Addison-Wesley, Menlo Park, CA.

Zucrow, M. J. and Hoffman, J. D., 1977, *Gas Dynamics*, Vol. II, John Wiley & Sons, Inc., New York.